EBioMedicine 63 (2021) 103163

Contents lists available at ScienceDirect

EBioMedicine

journal homepage: www.elsevier.com/locate/ebiom

Research paper

A novel imaging based Nomogram for predicting post-surgical biochemical recurrence and adverse pathology of prostate cancer from pre-operative bi-parametric MRI

Lin Li[a], Rakesh Shiradkar[a], Patrick Leo[a], Ahmad Algohary[a], Pingfu Fu[b], Sree Harsha Tirumani[c], Amr Mahran[d], Christina Buzzy[d], Verena C Obmann[e,f], Bahar Mansoori[g], Ayah El-Fahmawi[h], Mohammed Shahait[h], Ashutosh Tewari[i], Cristina Magi-Galluzzi[j], David Lee[h], Priti Lal[h], Lee Ponsky[d,k], Eric Klein[l], Andrei S. Purysko[l,m], Anant Madabhushi[a,n,*]

[a] Center for Computational Imaging and Personalized Diagnostics, Case Western Reserve University, Cleveland, OH, USA
[b] Department of Population and Quantitative Health Sciences, Case Western Reserve University, Cleveland, OH, USA
[c] Department of Radiology, University Hospitals, Cleveland, OH, USA
[d] Urology Institute, University Hospitals Cleveland Medical Center, Cleveland, OH, USA
[e] Department of Radiology, Case Western Reserve University and University Hospitals Cleveland Medical Centers, Cleveland, OH, USA
[f] Department of Diagnostic, Interventional and Pediatric Radiology (DIPR), Inselspital, Bern University Hospital, University of Bern, Switzerland
[g] Department of Radiology, Abdominal Imaging Division, University of Washington, Seattle, WA, USA
[h] Penn Medicine, University of Pennsylvania Health System, PA, USA
[i] Department of Radiology, Icahn School of Medicine at Mount Sinai, New York, New York, USA
[j] Department of Pathology, University of Alabama at Birmingham, AL, USA
[k] Case Western Reserve University School of Medicine, Cleveland, OH, USA
[l] Glickman Urological and Kidney Institute, Cleveland Clinic, Cleveland, OH, USA
[m] Imaging Institute, Cleveland Clinic, Cleveland, OH, USA
[n] Louis Stokes Cleveland Veterans Administration Medical Center, USA

ARTICLE INFO

Article History:
Received 3 September 2020
Revised 20 November 2020
Accepted 23 November 2020
Available online xxx

Keywords:
Prostate cancer
Biochemical recurrence
Adverse pathology
Radiomic
MRI
Prognosis

ABSTRACT

Background: We developed and validated an integrated radiomic-clinicopathologic nomogram (RadClip) for post-surgical biochemical recurrence free survival (bRFS) and adverse pathology (AP) prediction in men with prostate cancer (PCa). RadClip was further compared against extant prognostics tools like CAPRA and Decipher.
Methods: A retrospective study of 198 patients with PCa from four institutions who underwent pre-operative 3 Tesla MRI followed by radical prostatectomy, between 2009 and 2017 with a median 35-month follow-up was performed. Radiomic features were extracted from prostate cancer regions on bi-parametric magnetic resonance imaging (bpMRI). Cox Proportional-Hazards (CPH) model warped with minimum redundancy maximum relevance (MRMR) feature selection was employed to select bpMRI radiomic features for bRFS prediction in the training set (D_1, N = 71). In addition, a bpMRI radiomic risk score (RadS) and associated nomogram, RadClip, were constructed in D_1 and then compared against the Decipher, pre-operative (CAPRA), and post-operative (CAPRA-S) nomograms for bRFS and AP prediction in the testing set (D_2, N = 127).
Findings: "RadClip yielded a higher C-index (0.77, 95% CI 0.65-0.88) compared to CAPRA (0.68, 95% CI 0.57-0.8) and Decipher (0.51, 95% CI 0.33-0.69) and was found to be comparable to CAPRA-S (0.75, 95% CI 0.65-0.85). RadClip resulted in a higher AUC (0.71, 95% CI 0.62-0.81) for predicting AP compared to Decipher (0.66, 95% CI 0.56-0.77) and CAPRA (0.69, 95% CI 0.59-0.79)."
Interpretation: RadClip was more prognostic of bRFS and AP compared to Decipher and CAPRA. It could help pre-operatively identify PCa patients at low risk of biochemical recurrence and AP and who therefore might defer additional therapy.
Funding: The National Institutes of Health, the U.S. Department of Veterans Affairs, and the Department of Defense.

* Corresponding author at: Center for Computational Imaging and Personalized Diagnostics, 2071 Martin Luther King Drive, Cleveland, Ohio 44106-7207, Wickenden 523.
E-mail address: axm788@case.edu (A. Madabhushi).

https://doi.org/10.1016/j.ebiom.2020.103163

Research in Context

Evidence before this study

Prostate cancer (PCa) is the most common cancer among men. Approximately 20 to 40 percent of patients experience biochemical recurrence (BCR) following definitive therapy, and may further develop metastasis. Several tools, such as the Prostate Cancer Risk Assessment (CAPRA) score, Post-surgery Prostate Cancer Risk Assessment (CAPRA-S) score, and Decipher genomic test, have been proposed to identify patients who are at risk of developing BCR or adverse pathology (AP). AP is known to be strongly associated with risk of BCR and metastasis. Recently, radiomic features derived from bi-parametric magnetic resonance imaging (bpMRI) have been shown to capture sub-visual texture patterns for quantitative characterization of tumors phenotypes, and radiomic classifiers have been shown to aid in PCa risk stratification. Integrating pre-operative bpMRI derived radiomic parameters with clinicopathologic parameters may allow for even better prognostication of AP and PCa-specific outcome.

Added value of this study

In this study, we developed a prognostic nomogram, RadClip, and incorporated radiomic features extracted from bpMRI with pre-operative clinicopathologic parameters. Following an independent, multisite validation, we found that pre-operative RadClip was more prognostic of BCR and AP compared to Decipher and CAPRA for PCa patients who had undergone radical prostatectomy.

Implications of all the available evidence

The radiomic nomogram presented in this study could be potentially used as a surrogate to genomic-based prognostic tests to identify PCa patients with low risk of BCR and AP and who therefore might defer additional therapy.

Introduction

Radical prostatectomy (RP) is one of the primary treatments for localized prostate cancer (PCa) [1]. However, approximately 20% to 40% of patients experience biochemical recurrence (BCR) who may further develop metastasis after definitive treatment [2–4]. In addition, it has been shown that 25% of patients with low PCa volume and biopsy Gleason Grade Group (GG) 2 harbor adverse pathology (AP) [5], which is known to be a predictor for developing BCR and subsequent metastasis [6,7], and thus indicates exclusion of active surveillance [8].

Several tools have been proposed to identify patients at risk of presence of AP at final pathology [8], developing BCR [9,10], and subsequent metastasis [9–11]. These have included pre-operative tools, such as Prostate Cancer Risk Assessment (CAPRA) score, which was used to predict AP, risk of BCR and metastasis, and prostate cancer–specific survival [10]; and post-operative tools like Post-surgery Prostate Cancer Risk Assessment (CAPRA-S) score, which was developed to predict risk of BCR and metastasis after RP [9]. These assessments integrate factors, such as prostate–specific antigen (PSA), GG, surgical margin (SM) status, extracapsular extension (EPE), seminal vesicle invasion (SVI), and lymph node involvement (LNI), which have been previously shown to be significantly associated with risk of BCR [9]. However, these tools based on clinicopathological features failed to account for tumor molecular heterogeneity and their performance varies between different cohorts. In the last decade, there has been heightened interest in exploring the utility of different genomic signatures in predicting oncological outcomes after RP; the most utilized test in the real world practice is Decipher which has been shown to correlate with increased cumulative incidence of BCR, metastasis and PCa-specific mortality [12].

Pre-operative multi-parametric magnetic resonance imaging (mpMRI) has been utilized to help in PCa diagnosis [13], planning for surgery [14] and to predict the presence of AP, e.g. SVI [15] and EPE [16]. Recently, mpMRI radiomic derived features have shown to capture of sub-visual texture patterns for quantitative characterization of tumors phenotypes, and help in PCa risk stratification [17–20]. Integrating pre-operative mpMRI derived radiomic parameters with clinicopathologic parameters may allow for even better prognostication of AP and PCa specific outcome.

In this study, we sought to develop and evaluate a radiomic risk score (RadS) derived from bi-parametric MRI (bpMRI), including T2-weighted (T2WI) and Diffusion Weighted Imaging (DWI), for prediction of biochemical recurrence free survival (bRFS) and AP. Additionally, we also constructed a novel nomogram, RadClip, by integrating RadS, pre-operative prostate-specific antigen (PSA) and biopsy GG. RadClip was compared against the Decipher test, and the pre-operative CAPRA and post-operative CAPRA-S nomograms for bRFS and AP prediction on a multi-site validation set.

Materials and methods

Ethics statement

This retrospective study was approved by the Case Western Reserve University Institutional Review Board reviews (IRB) and was compliant with the Health Insurance Portability and Accountability Act (HIPAA); de-identified data were used, and no protected health information was needed. The need for an informed consent from all patients was waived by the IRB.

Patient selection

A total of 408 PCa patients from four institutions who had undergone pre-operative 3 Tesla (3T) prostate mpMRI between 2009 and 2017 were initially identified. Patients who met the following criteria were selected: patients who had (1) undergone RP after the MRI; (2) no history of neoadjuvant or adjuvant therapy; (3) images of adequate quality; and (4) and follow up information which includes postoperative serum PSA measurements (Fig. 1). Patients were excluded if they (1) were without T2WI or Apparent Diffusion Coefficient (ADC) maps; (2) were of sub-optimal image quality, e.g. ADC map distortion; (3) received radiation therapy (RT) as the definitive treatment, due to the difference in definition of BCR between RP and RT [2–4]; (4) were with PSA persistence; or (5) received additional therapies before RP.

A total of 198 patients that met the above eligibility criteria with a median follow-up of 35 months were identified, of these 106 men also underwent the Decipher test on PCa tissue sampled from the corresponding surgical specimen. (Table 1) 71 patients from a single site comprised the training set (D_1), the remaining patients comprised the independent test set (D_2, N=127).

BCR was defined as 2 consecutive serum PSA > 0.2 ng/mL; bRFS was defined as the interval between the date of RP and the date of BCR [21]. Patients who were still alive without BCR at the last reported follow-up or the date of additional therapy applied were labeled as censored. AP was defined as the presence of SVI, EPE or LNI on the surgical specimen.

MRI Protocol and prostate cancer delineations

All patients were imaged on 3T MRI scanners with either a surface pelvic phased-array coil (PPAC) or an endorectal coil (ERC). All studies

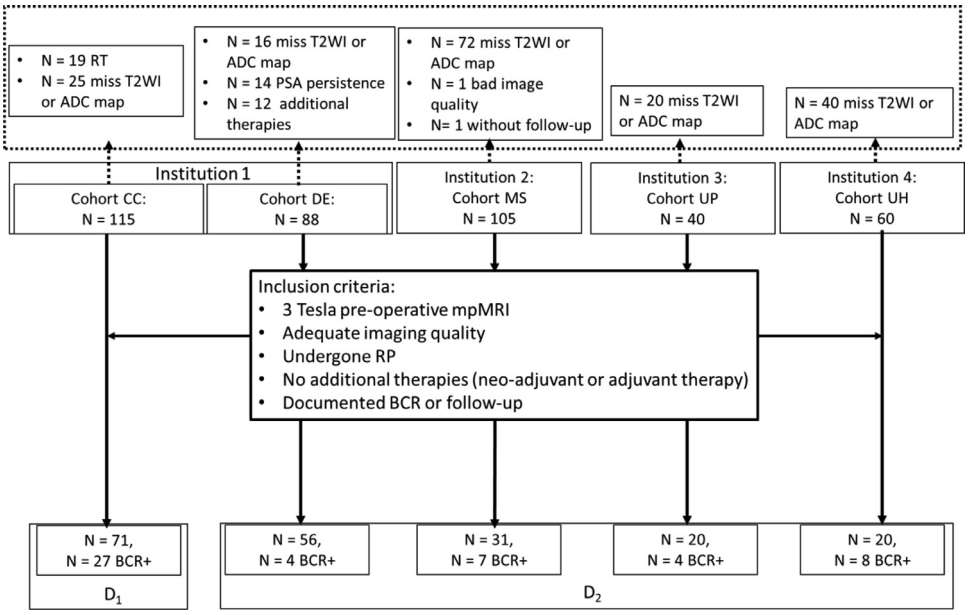

Fig. 1. Flowchart of patient selection from four institutions. RT = radiation therapy; RP = radical prostatectomy; BCR = biochemical recurrence; mpMRI = multi-parametric magnetic resonance imaging.

included axial turbo spin-echo T2WI and axial DWI with ADC maps at minimum. (Table 2) The mpMRI scans were reviewed and PCa regions were delineated on T2WI and ADC maps using the 3D Slicer software [22] by experienced radiologists. (A.S.P, 10 years of experience; V.C.O, 4 years of experience, S.H.T, 7 years of experience; and B. M 2 years of experience) The PCa delineations on MRI were made either by referring to their corresponding RP specimen (N = 56), or biopsy and pathology reports when RP specimens were not available (N = 142). Only the index lesions, defined as tumor of highest GG from each patient were included for radiomic analysis.

MRI pre-processing and radiomic analysis

Intensity drift artifacts across different MRI acquisitions cause T2WI to lack in tissue-specific meaning. Therefore, a nonparametric intensity standardization method [23] was used to align T2WI intensity distributions. In addition, bias-field artifacts introduced by the endorectal coil were corrected using a previously published method in which the estimated bias field is subtracted from the acquired image data [24]. Both T2WI and ADC maps were resampled to the same spatial resolution in the axial plane (0.5×0.5mm). After preprocessing, 200 radiomic feature, including first and second order statistics, Gabor [25], Laws [26], Haralick [27] and CoLlAGe features [28], were extracted on a per-voxel basis within PCa lesion regions on both T2WI and ADC maps. These features characterize the underlying texture, quantify heterogeneity on imaging, and have previously been shown to be promising in PCa characterization [17,29,30]. Statistics including mean, standard deviation, skewness, and kurtosis were calculated for each voxel-wise radiomic feature to characterize its distribution within each PCa lesion region.

Statistics

Feature selection and stability assessment. Highly correlated (Pearson's correlation coefficient (R) $>$ 0.9) radiomic features were first eliminated and unstable radiomic features were further excluded using test-retest scans from the Quantitative Imaging Network (QIN) [31]. This dataset involved test-retest 3T mpMRI scans of 15 subjects obtained over a period of 2 weeks using the same scanner with PCa lesions annotated separately on each scan [31]. The rationale behind using these QIN cases was that stable radiomic features should remain relatively consistent across the test-retest scans of the same patient. Consequently, we only included stable radiomic features which are identified as those without significant difference ($p <$ .05, Wilcoxon signed-rank test) between the test-retest scans. Minimum Redundancy Maximum Relevance (mRMR) [32] feature selection with multivariable Cox-Proportional Hazards (CPH) model was employed to identify the set of radiomic features and corresponding CPH model that produced highest C-index for bRFS prediction on D_1. The top 5 most frequently selected radiomic features across multiple iterations of 5-fold and 10-run cross-validation were employed to construct the radiomic model producing a radiomic risk score (RadS) to estimate bRFS. Moreover, a radiomic-clinicopathologic nomogram (RadClip), integrating RadS and pre-operative PSA and biopsy GG, was constructed based on the multivariable CPH model for 3-year bRFS prediction. (Fig. 2) RadClip and RadS were both constructed using the rms packages in R software version 3.6.

Validation. RadS was then evaluated on D_2. Both the univariable and multivariable CPH models were fitted with RadS and clinicopathologic parameters, including biopsy GG, Prostate Imaging-Reporting and Data System version 2 (PI-RADS v2) score [33], age, pre-operative PSA, and clinical stage (cT, T2 or T3), to evaluate the role of radiomic features in the prediction of bRFS after RP. A head-to-head comparison between RadClip, Decipher, CAPRA, and post-surgical CAPRA-S score was conducted on subgroups of patients in D_2 for bRFS prediction, who either underwent Decipher test (N = 106) or had sufficient information to calculate the CAPRA (N =106) or CAPRA-S (N = 121) scores, in terms of concordance index (C-index) and Kaplan-Meier curves. Both Decipher risk score, ranging 0-1, and Decipher risk groups (low risk group with Decipher risk score $<$ 0.4, intermediate 0.4-0.6, high $>$ 0.6) [12] were included for comparison. Hazard ratios (HRs) of the multivariable CPH model indicate the influence of corresponding predictors. Wald test was applied and P values under .05 were considered to be statistically significant. Decision curve analysis was adopted to calculate the net benefit for RadClip, CAPRA score and CAPRA-S score in comparison to default strategies of treating all or no patients [34]. Area under receiver operating characteristic curve (AUC) was used to evaluate association between AP and pre-

Table 1
Demographic and disease characteristics of all 198 study patients.

Dataset	D_1Training	D_2Validation			
Cohort	CC	MS	UP	UH	DE
# patients	71	31	20	20	56
Median age, (range)	59 (47-79)	63 (48-73)	64 (49-73)	61 (47-86)	64 (42-76)
Mean pretreatment PSA ± SD, ng/mL (range)	10.0 ± 10.9 (1 - 53.8)	8.8 ± 5.0 (3.7 - 22.5)	6.0 ± 1.6 (4.2 - 8.9)	10.6 ± 18.5 (1.8 - 88.3)	9.0 ±12.1 (1.2-69.4)
Biopsy GG, n/# patients (%)					
1	15/71 (21.13)	0/31 (0)	0/20 (0)	3/20 (15)	7/56 (12.50)
2	20/71 (28.17)	15/31 (48.39)	14/20 (70)	6/20 (30)	27/56 (48.21)
3	8/71 (11.27)	9/31(29.03)	4/20 (20)	5/20 (25)	13/56 (23.21)
4	10/71 (14.08)	2/31 (6.45)	1/20 (5)	4/20 (20)	3/56 (5.36)
5	18/71 (25.35)	5/31 (16.13)	1/20 (5)	2/20 (10)	6/56 (10.71)
Pathologic GG, n/# patients (%)					
1	6/71 (8.45)	0 /31 (0)	0/20 (0)	3/20 (15)	4/56 (7.14)
2	22/71 (30.99)	15/31 (48.39)	13/20 (65)	8/20 (40)	24/56 (42.86)
3	13/71 (18.31)	13/31 (41.94)	5/20 (25)	4/20 (20)	15/56 (26.79)
4	7/71 (9.86)	1 /31 (3.23)	1/20 (5)	2/20 (10)	3/56 (5.36)
5	18/71 (25.35)	2 /31 (6.45)	1/20 (5)	3/20 (15)	10/56 (17.86)
NA	5/71 (7.04)				
PI-RADS v2, n/# lesions (%)					
1	0/71 (0)	0/31	0/20	0/20 (00)	1/56 (1.79)
2	10/71(14.08)	0/31	0/ 20	2/20 (10)	8/56 (14.29)
3	6/71(8.45)	1/31 (3.23)	6/20 (30)	2/20 (10)	3/56 (5.36)
4	20/71(28.17)	17/31 (54.84)	8/20 (40)	6/20 (30)	10/56 (17.86)
5	34/71(47.89)	13/31 (41.94)	6/20 (30)	10/20 (50)	34/56 (60.71)
NA	1/71(1.41)				
Decipher risk categories, n/# patients (%)					
Low	NA	16/31 (51.61)	6/20 (30)	NA	23/56 (41.07)
Intermediate	NA	8/31 (25.81)	8/20 (40)	NA	5/56 (8.93)
High	NA	7/31 (22.58)	5/20 (25)	NA	28/56 (50)
NA	NA	0/31 (0)	1/20 (5)	NA	0/56 (0)
CAPRA, n/# patients (%)					
Low	NA	4/31 (12.90)	NA	4/20 (20)	4/56 (7.14)
Intermediate	NA	17/31 (54.84)	NA	9/20 (45)	38/56 (67.86)
High	NA	9/31 (29.03)	NA	7/20 (35)	14/56 (25.00)
NA	NA	1/31 (3.23)	NA	0/20 (0)	0/56 (0)
CAPRA-S, n/# patients (%)					
Low	NA	11/31 (35.48)	NA	4/20 (20)	16/56 (28.57)
Intermediate	NA	16/31 (51.61)	NA	10/20 (50)	17/56 (30.36)
High	NA	4/31 (12.90)	NA	5/20 (25)	20/56 (35.71)
NA	NA	0/31 (0)	NA	1/20 (5)	3/56 (5.36)
BCR n/# patients (%)					
BCR+	27/71 (38.03)	6/31 (19.35)	4/20 (20)	8/20 (40)	4/56 (7.14)
BCR-	44/71 (61.97)	25/31 (80.65)	16/20 (80)	12/20 (60)	52/56 (92.86)
BCR+ median follow-up / mon.	11.1	2.6	12.5	8.5	13.2
BCR- median follow-up / mon.	64.8	20.6	25	33.5	27.9
SVI, n/# patients (%)					
Yes	24/71 (33.80)	4/31 (12.90)	2/20 (10)	4/20 (20)	16/67 (23.88)
No	42/71 (59.15)	27/31 (87.09)	18/20 (90)	16/20 (80)	51/67 (76.12)
Not determined	5/71 (7.04)	0/31 (0)	0/20 (0)	0/20 (0)	0/67 (0)
EPE, n/# patients (%)					
Yes	33/71 (46.48)	10/31 (32.26)	10/20 (50)	8/20 (40)	42/67 (62.69)
No	30/71 (42.25)	21/31 (67.74)	10/20 (50)	12/20 (60)	25/67 (37.31)
Not determined	8/71 (11.27)	0/31 (0)	0/20 (0)	0/20 (0)	0/67 (0)
LNI, n/# patients (%)					
Yes	12/71 (16.90)	3/31 (9.68)	NA	1/20 (5)	20/67 (29.85)
No	41/71 (57.75)	28/31 (90.32)	NA	18/20 (90)	42/67 (62.69)
Not determined	18/71 (25.35)	0/31 (0)	NA	1/20 (5)	5/67 (7.46)
PSM, n/# patients (%)					
Yes	NA	1/31 (3.23)	19/20 (95)	6/20 (30)	33/67 (49.25)
No	NA	30/31 (96.77)	0/20 (0)	14/20 (70)	34/67 (50.75)
Not determined	NA	0/31 (0)	1/20 (5)	0/20 (0)	0/67 (0)
cT, **n/# patients (%)**					
T1	NA	15/31 (48.39)	18/20 (90)	8/20 (40)	53/67 (79.10)
T2	NA	14/31 (45.16)	1/20 (5)	9/20 (45)	14/67 (20.90)
T3	NA	1/31(3.23)	1/20 (5)	3/20 (15)	0 (0)
NA	0 (0)	1/31 (3.23)	0 (0)	0 (0)	0 (0)

PSA = prostate-specific antigen, GG = Grade Group, PI-RADS v2 = Prostate Imaging Reporting and Data System version 2, BCR = Biochemical Recurrence, SVI = Seminal Vesicle Invasion, EPE = Extra Prostatic Extension, LNI = Lymph Node Invasion, PSM = Positive Surgical Margin, cT = clinical stage, NA = Not Available.

operative prognostic models RadClip, CAPRA, and Decipher on D_2. We also evaluated the association between RadClip and the presence of SVI, EPE or LNI separately, and then compared RadClip with CAPRA, CAPRA-S, and Decipher in terms of AUC.

Role of the funding source

The sponsors of this study had no role in the research design, data collection, data analysis, data interpretation, and paper writing. The

Table 2
MRI scan parameters.

Parameter	Institution 1 Scanner 1	Scanner 2	Institution 2 Scanner 1	Institution 3 Scanner 1	Institution 4 Scanner 1
Manufacturer	Philips Medical Systems, Best, Netherlands	Siemens Healthcare, Erlangen, Germany	Siemens Healthcare, Erlangen, Germany	Siemens Healthcare, Erlangen, Germany	Siemens Healthcare, Erlangen, Germany
Model	3T Achieva	3T Skyra	3T Skyra	3T Skyra	3T Skyra
Coils	ERC	PPAC	PPAC	ERC	PPAC
T2WI					
TR/TE	3802–5151/105–115	3730/121	5610/121	3000-6000/ 80-120	7200/96
Reconstruction voxel size (mm^3)	0.3 × 0.3 × 3.0	0.5 × 0.5 × 3.0	0.3 × 0.3 × 3.0	0.3 × 0.3 × 3.0	0.6 × 0.6 × 3.0
Acquisition time (min)	5.36	2.53	2.54	4-5	2.25
DWI					
TR/TE	3571–4880/50–74	4700/86	8700/72		7900/88
Reconstruction voxel size (mm^3)	1.4 × 1.4 × 3.0	1.6 × 1.6 × 3.0	2.2 × 2.2 × 3	1.4 × 1.4 × 3.0	1.2 × 1.2 × 3.0
b–values (s/mm^2)	0, 500, 1000, 1500, 2000	0, 400, 900, 1500	50,1000,1600,2000	0, 1000, 1400	50, 600, 1000, 1400
Acquisition time (min)	5.25	5.07	2.57	3-6	2.34

TR = repetition time, TE = echo time, T2WI = T2-weighted imaging, DWI = diffusion-weighted imaging, PPAC = pelvic phased-array coil, ERC = endorectal coil.

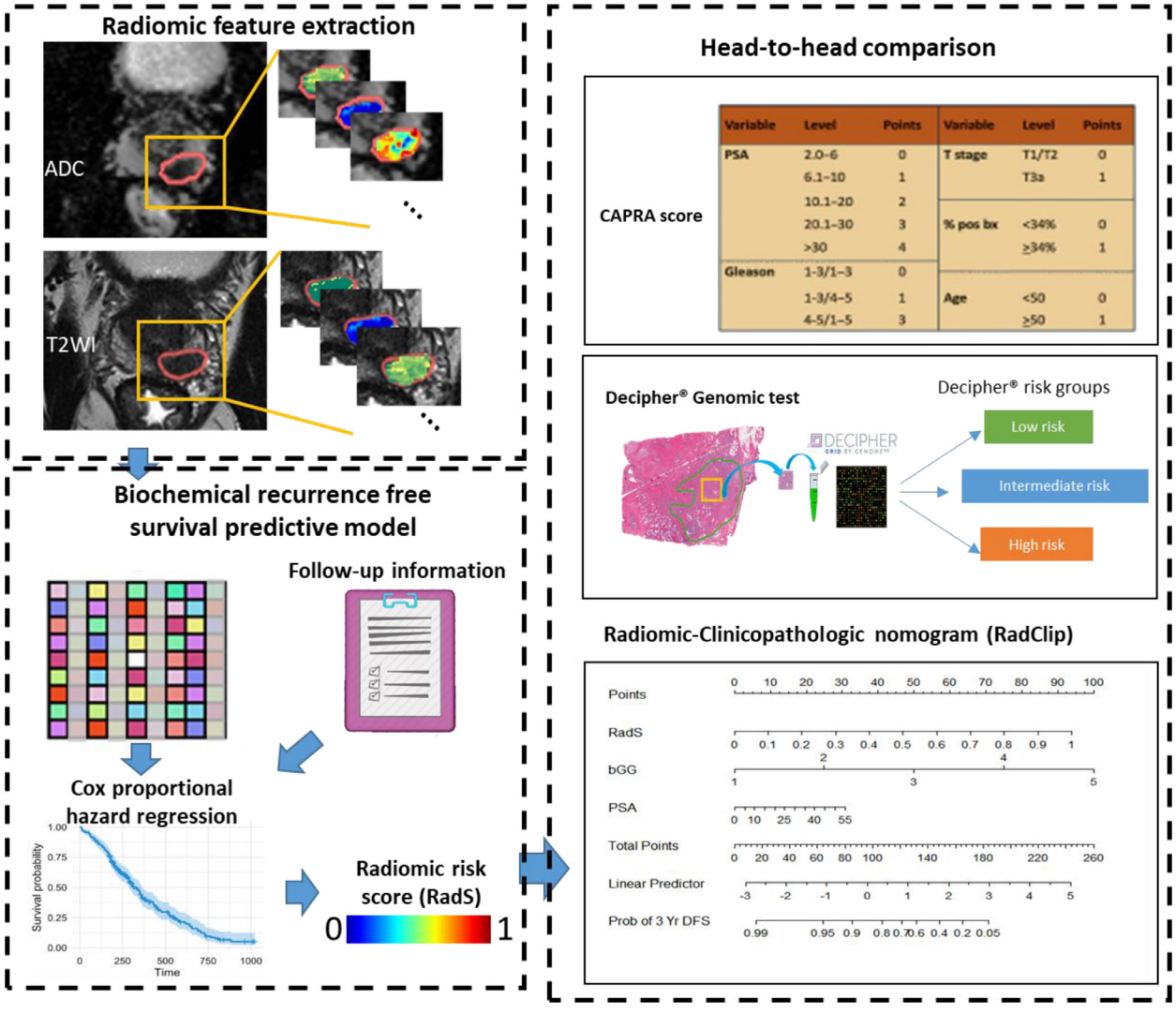

Fig. 2. overall workflow and pipeline. T2WI = T2-weighted magnetic resonance imaging; ADC = apparent diffusion coefficient.

corresponding authors had full access to all data obtained from this study and had final responsibility for the decision to submit for publication.

Results

Ability of radiomic model to predict bRFS

RadS was built with 5 radiomic features selected within D_1. (Table 3 and Fig. 3) RadS on D_2 resulted in an HR = 7.01 (95% CI, 1.21 − 40.68, p < .05) on multivariable analysis. RadS was significantly associated with bRFS and found to be prognostic independent of other pre-operative clinicopathologic parameters, including biopsy GG, PI-RADS v2, age, pre-operative PSA, and cT, to predict bRFS. (Table 4).

Ability of RadClip to predict bRFS and head-to-head comparisons

The prognostic performance of RadClip was validated on D_2, resulting in a HR of 1.9 (95% CI, 1.4-2.7, p < .05) and C-index of 0.77 (95% CI, 0.65-0.88). For the patients in D_2, neither the Decipher risk score (C-index 0.51, 95% CI 0.33-0.69, N=106) nor associated risk groups (C-index 0.5, 95% CI 0.35-0.65, N=106) showed any significant association with bRFS in univariable analysis. (Table 5) RadClip achieved a higher C-index than CAPRA (0.77 vs. 0.68, N=106) and a similar C-index to CAPRA-S (0.77 vs. 0.75, N=121). (Table 3) In addition, RadClip illustrated significant association with bRFS independent of CAPRA, CAPRA-S and Decipher in the multivariable analysis. (Table 5) Furthermore, RadClip yielded a similar net benefit compared to CAPRA and CAPRA-S across decision threshold probabilities ranging from 20-30% [2,3,21] (Fig. 4)

Table 3
Biochemical-recurrence-associated Radiomic features.

Radiomic feature	Radiomic feature description
T2WI Laws feature	Wave texture distribution kurtosis
T2WI Laws feature	Wave-ripple texture distribution kurtosis
T2WI intensity range	Local intensity range distribution kurtosis
T2WI Haralick Information measure 1	Intensity heterogeneity distribution kurtosis
ADC Laws feature	Wave and edge texture distribution kurtosis

T2WI = T2-weighted imaging, ADC = apparent diffusion coefficient.

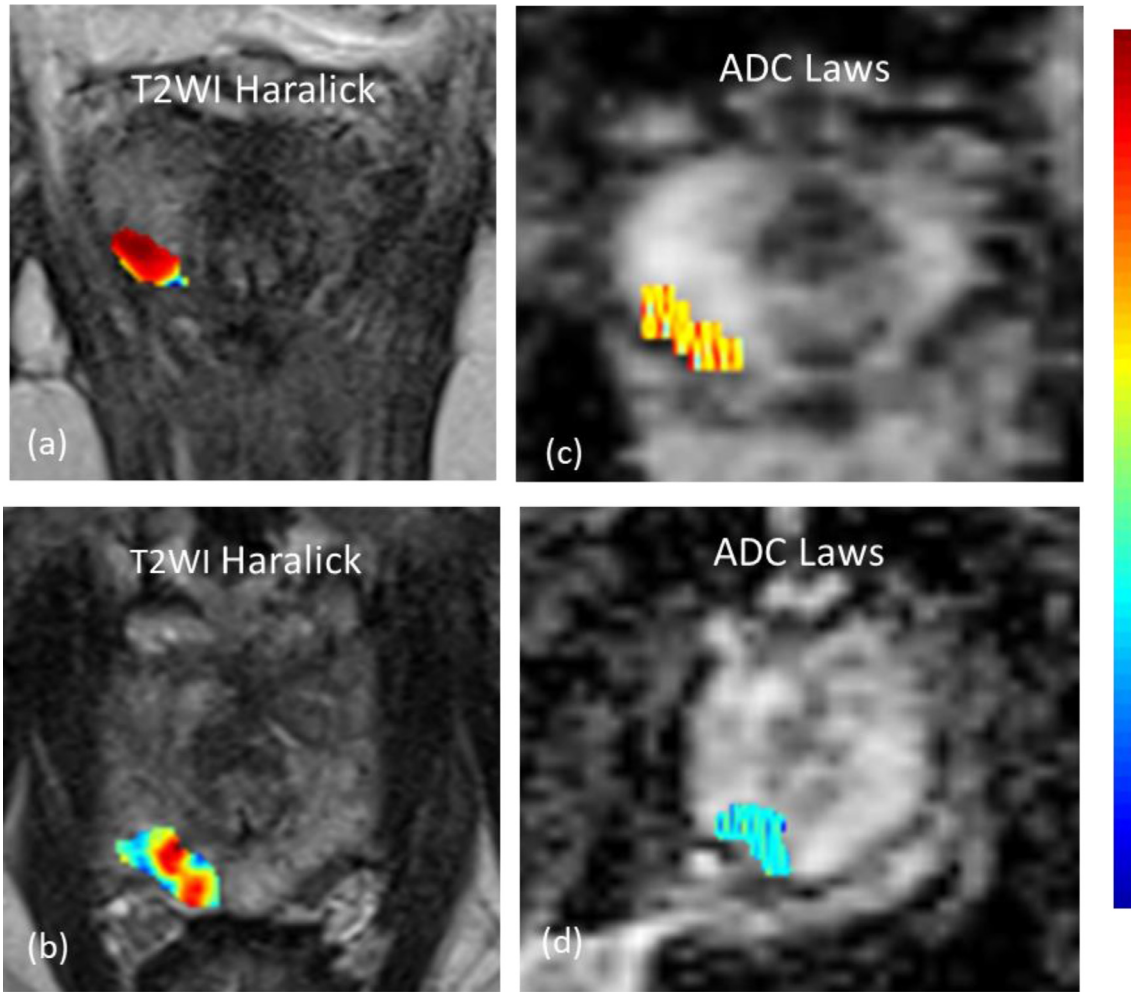

Fig. 3. BCR-associated Radiomic features. (**a**) and (**c**) are the bpMRI of a 59-year-old patient with BCR identified at 41-month follow-up. The patients had pathologic Gleason Grade Group = 2, PIRADS v2 = 2, Decipher risk score = 0.52, CAPRA score = 3, CAPRA-S score = 2, no adverse pathology identified. (**b**) and (**d**) are the bpMRI of a 62-year-old patient with no BCR identified at 45-month follow-up. The patient had pathologic Gleason Grade Group = 2, PIRADS v2 = 4, Decipher risk score = 0.63, CAPRA score = 3, CAPRA-S score = 4, no adverse pathology identified. (**a,b**) T2WI Haralick information measures; (**c,d**) ADC Laws feature capturing wave-edge pattern. BCR = biochemical recurrence; bpMRI = bi-parametric magnetic resonance imaging; PIRADS v2 = Prostate Imaging-Reporting and Data System version 2; CAPRA = Prostate Cancer Risk Assessment; CAPRA-S = Post-surgery Prostate Cancer Risk Assessment; T2WI = T2-weighted magnetic resonance imaging; ADC = apparent diffusion coefficient.

Table 4
Multivariable Biochemical-Recurrence-Free Survival analysis (N = 127, 22 BCR +)

Parameter name	Multivariable HR (95% CI)	Multivariable C-index (95% CI)	Multivariable p value
Biopsy GG	1.67 (1.09 -2.57)	0.79 (0.69-0.88)	0.02*
PI-RADS	0.99 (0.53-1.84)		0.97
PSA	1.04 (1.00-1.08)		0.071
Age	0.92 (0.85 – 0.98)		0.013*
Clinical Stage	1.92 (0.91 – 4..04)		0.087
RadS	7.01 (1.21 – 40.68)		0.03*

Table 5
Head to head comparison between RadClip, CAPRA and Decipher in BCR prediction.

RadClip, RadS and CAPRA (N = 106,18 BCR+) Model	HR (95% CI)	C-index (95% CI)	Univariable p-value	Multivariable p-value
RadClip	1.9 (1.4-2.7)	0.77 (0.65-0.88)	<0.001*	0.012*
CAPRA	1.4 (1.1-1.9)	0.68 (0.57-0.8)	0.007*	0.336

RadClip, RadS, and CAPRA-S (N = 121, 21 BCR+)				
RadClip	2 (1.5-2.8)	0.77 (0.66-0.87)	<0.001*	0.011*
CAPRA-S	1.4 (1.2-1.6)	0.75 (0.65-0.85)	<0.001*	0.046*

RadClip and Decipher (N = 106, 14 BCR+)				
RadClip	1.6 (1.1-2.4)	0.73 (0.59-0.87)	0.033*	0.041*
Decipher score	2.5 (0.17-37)	0.51 (0.33-0.69)	0.51	0.73
Decipher risk group	1.1 (0.61-2)	0.5 (0.35-0.65)	0.74	0.77

Association between pre-operative prognostic models and AP

We evaluated the association between RadClip and AP among patients from the validation set with EPE, SVI, and LNI specific information. RadClip yielded an AUC = 0.71 (95% CI, 0.62-0.81, $p < .05$) in predicting AP, compared to CAPRA, AUC = 0.69 (95% CI, 0.59-0.79, $p < .05$), and Decipher, AUC = 0.66 (95% CI, 0.57-0.77, $p < .05$), on D_2. In addition, RadClip had a higher AUC compared with CAPRA and Decipher in predicting EPE, SVI and LNI (Table 6).

Discussion

The ability to predict prognosis of prostate cancer (PCa) patients using pre-operative imaging and clinicopathologic parameters may allow for identification of patients who are more likely to have adverse pathologic factors, such as extracapsular extension (EPE), seminal vesicle invasion (SVI), and lymph node involvement (LNI). This could allow for identifying men who are not candidates for active surveillance (AS), but rather candidates for more aggressive treatments. Additionally, since the benefit of adjuvant radiation therapy is subject to debate [35], pre-operatively identifying patients with low risk of developing BCR after surgery could give clinicians more confidence in deferring additional treatments in these men. In this study, we developed a novel radiomic risk score, RadS, derived from computerized texture features from pre-surgical bi-parametric MRI that was shown to be independently prognostic of biochemical recurrence free survival (bRFS). Additionally, we presented RadClip, a pre-operative nomogram that combines radiomic features with clinicopathologic parameters (including biopsy Gleason Grade Group and pre-surgical PSA) to predict bRFS, as well as AP.

Results from our study indicate that Haralick features extracted from pre-operative T2WI and Laws features derived from both T2WI and ADC map showed significant differences between patients with and without BCR. Haralick features [27] capture spatial intensity based heterogeneity and Laws [26] features capture edge and wave texture patterns on MRI. Haralick features of PCa on T2WI have been previously shown to be associated with biochemical recurrence (BCR) [17,29], men who had BCR following surgery tended to have a higher expression of Haralick features within the tumor on pre-operative T2WI versus those who did not. Additionally, Laws features derived from prostate bpMRI lesion regions have also been shown to be associated with PCa aggressiveness, in particular with RP Gleason grade [30]. We observed that patients with poor prognosis tended to have higher expression of T2WI Haralick feature and edge and wave texture within tumor regions on ADC maps, suggesting a higher degree of morphologic disease specific heterogeneity. (Fig. 3 and Table 3)

In our study, the performance of both CAPRA and CAPRA-S for the task of bRFS prediction was found to be consistent to results reported in previous studies [10]. RadClip, as a pre-operative prognostic nomogram was found to outperform CAPRA score and achieve similar performance as the post-surgical CAPRA-S score in a head-to-head comparison for bRFS prediction. These results illustrated the potential of RadClip to predict prognosis pre-operatively which will allow for identification of patients who could potentially benefit from receiving neo-adjuvant therapy. In addition, RadClip also showed strong association with AP, suggesting its possible utility in pre-operative identification of men with PCa who should likely be excluded from consideration for active surveillance.

While the Decipher test has been previously validated in its ability to predict risk of metastasis and PCa specific mortality [12,36], in our study the test did not show a significant association with bRFS. This may have been because the Decipher test was initially validated to predict risk of metastasis and not BCR per se [11]. Interestingly, a previous study [36] also appeared to corroborate our findings, suggesting that the Decipher risk score did not have a strong association with post-surgical BCR. Decipher was shown to have significant association with AP in our validation cohort. However, note that in this study, Decipher was performed post-surgically on the resected specimen, unlike RadClip which was assessed pre-operatively. Although a previous study has suggested that Decipher estimated on biopsy tissue was similar to the corresponding score estimated on the surgical specimens [37], the biopsy sampling error may still be a concern indicating by another study as no correlation between Decipher score estimated from index lesions and benign regions [38]. Unlike Decipher, RadClip is also completely tissue non-destructive and is not constrained by the limitations of biopsy sampling errors. Also, since RadClip only requires diagnostic mpMRI, the test does not consume tissue like molecular tests like Decipher. We acknowledge the fact that post-surgery Decipher test is usually reserved for patients with T2 and positive surgical margins, T3a/b, PSA persistence, and in selected cases of BCR; therefore, the comparison between RadClip and Decipher may seem counter-intuitive but it reflects over-utilization of Decipher test in this population as 45/106 patients had low risk score.

The application of assessing the association between mpMRI derived parameters, e.g. PI-RADS v2 score or lesion volume, with BCR, PCa aggressiveness and molecular tests like Decipher is not new [39,40]. Jambor et. al. illustrated that combing clinicopathologic parameters with mpMRI was comparable in prediction of BCR as a combination of Decipher and clinicopathologic parameters [40]. This study was however limited in its sample size, single institutional design and the fact that PI-RADS is known to be subject to inter-reader variability [41]. Similarly, Shiradkar et. al. illustrated using bpMRI derived radiomic features could be prognostic of BCR [17]. However, this study too was limited to scans from a single site in their validation set. Our study differed from previous studies [17–20,29] in a few different ways. Firstly, instead of investigating the correlation between radiomic features and Decipher risk categories or pathologic Gleason Grade [18], we directly built a nomogram

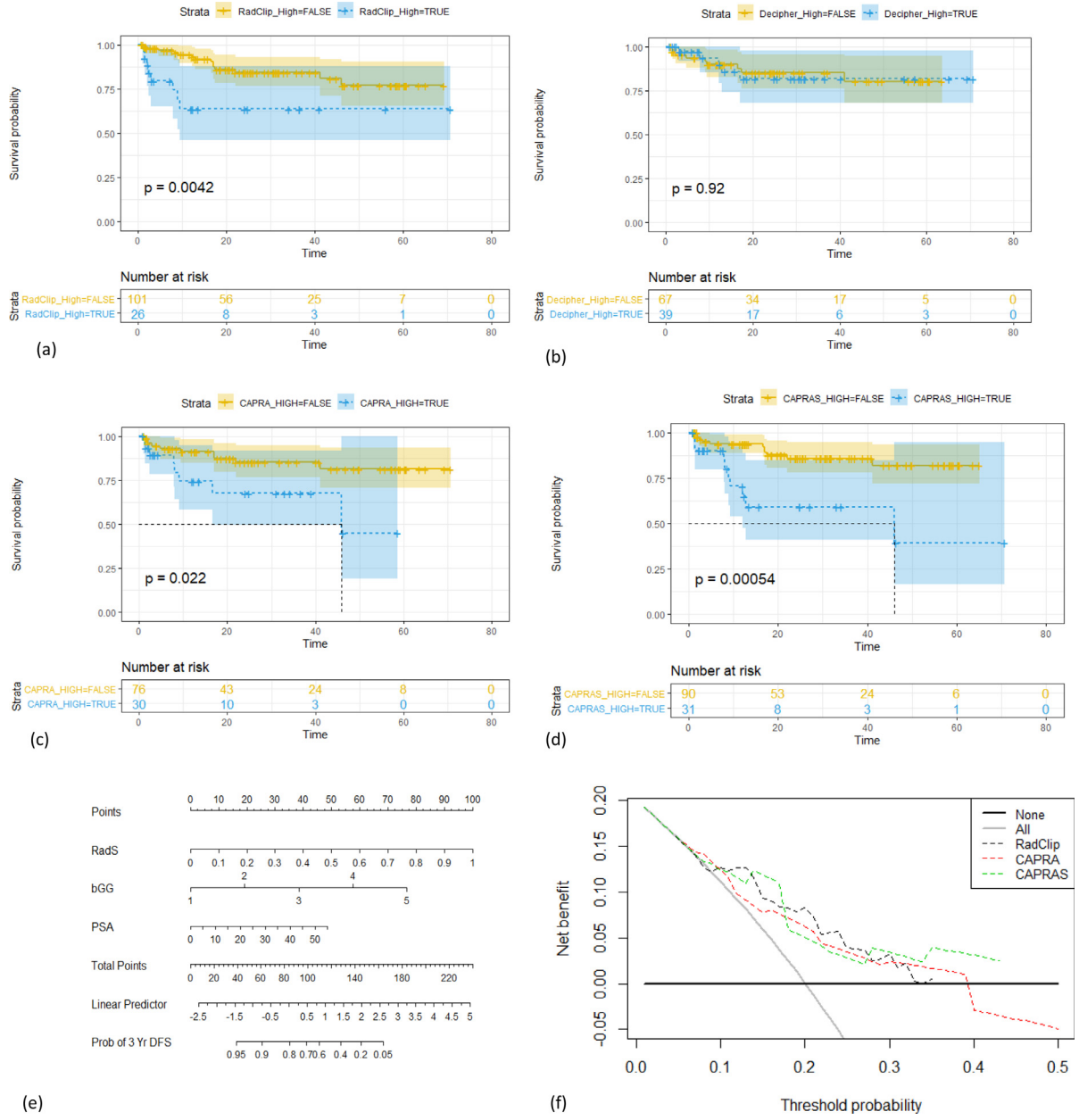

Fig. 4. Biochemical-recurrence-free survival analysis. (**a**) Kaplan-Meier survival analysis of RadClip (N = 127) with the cut-off point at 70% 3-year Biochemical-recurrence-free survival. (**b**) Kaplan-Meier survival analysis of Decipher score (N = 106). Decipher score > 0.6 is defined as the high risk category. (**c**) Kaplan-Meier survival analysis of CAPRA score (N = 106). CAPRA score ≥ 6 is defined as the high risk. (**d**) Kaplan-Meier survival analysis of CAPRA-S score (N = 121). CAPRA-S score ≥ 6 is defined as the high risk. (**e**) 3-year biochemical recurrence-free radiomic-clinicopathologic nomogram (RadClip) built with radiomic risk score (RadS), biopsy Grade Group (bGG), pre-operative prostate-specific antigen (PSA). (**f**) Decision curve showing net benefit for carrying out adjuvant therapy in prostate cancer patients. It has been shown that 20-30% patients will develop BCR after RP within 10 years. Black dash line represents RadNom showing increment of the net benefit compared CAPRA score (red) and CAPRA-S score (green).

to predict clinical endpoints, e.g. BCR and AP. In addition, unlike previous approaches that have attempted to directly train radiomic classifiers against binary outcome (e.g. presence or absence of BCR) [17,29,40], our approach employed a Cox proportional hazards approach to build an imaging based prognostic model accounting for time to BCR as also censoring information introduced by the variance of follow-up time among patients. Moreover, this was also one of the very few studies we are aware of to validate an MRI based PCa prognostic tool in a multi-institutional setting [19,29,40]. The findings of RadClip on scans from 4 institutions, suggest that the approach is

Table 6
Head to head comparison between RadClip, CAPRA and Decipher in Adverse Pathology prediction (N = 127).

Model	EPE, AUC (95% CI)N = 60, EPE +	SVI, AUC (95% CI)N = 21, SVI +	LNI, AUC (95% CI)N = 19, LNI +	Adverse Pathology, AUC (95% CI)N = 66 AP +
RadClip	0.7 (0.61-0.8)	0.82 (0.74-0.91)	0.77 (0.67-0.86)	0.71 (0.62-0.81)
CAPRA	0.69 (0.59-0.79)	0.76 (0.65-0.86)	0.74 (0.62-0.85)	0.69 (0.59-0.79)
Decipher risk score	0.68 (0.58-0.78)	0.77 (0.65-0.9)	0.73 (0.59-0.87)	0.66 (0.56-0.77)

relatively robust and resilient to scanner and site-specific MRI variations.

We acknowledge however that our study did have its limitations. First, implicit bias may exist due to the retrospective nature of the study; however, the multi-institutional validation suggests the robustness of RadClip. In addition, even though 198 patients were included in this study, this number is actually larger compared to other recent related studies [17,18,40]. However, we acknowledge that prior to clinical deployment, the approach needs additional retrospective and potentially prospective clinical trial validation in the future to further confirm the generalizability of our findings. Second, this study employed BCR as a surrogate endpoint for metastasis because of insufficient follow-up time after RP, as opposed to metastasis. Furthermore, we demonstrated that the nomogram was prognostic and not predictive of added benefit of neoadjuvant or adjuvant therapy, though that it will certainly be included for our future work. Also, an automated lesion detection and segmentation module on the MRI scans could be implemented in consort with RadS and RadClip in future.

In spite of these limitations, our study suggests that with additional independent multi-site validation, these radiomic features could potentially be used for pre-operative risk stratification in patients with PCa to allow for more effective treatment management.

Conclusion

In this study, we developed a prognostic nomogram, RadClip, integrating radiomic features derived from pre-operative biparametric MRI, biopsy GG and pre-operative PSA to predict biochemical recurrence free survival and adverse pathology in prostate cancer patients undergoing prostatectomy. RadClip outperformed Decipher risk score and CAPRA score on a limited hold-out validation set.

Declaration of Competing Interests

Dr. Madabhushi is an equity holder in Elucid Bioimaging and in Inspirata Inc. In addition, he has served as a scientific advisory board member for Inspirata Inc, Astrazeneca, Bristol Meyers-Squibb and Merck. Currently he serves on the advisory board of Aiforia Inc. He also has sponsored research agreements with Philips, AstraZeneca and Bristol Meyers-Squibb. He has 15 relevant issued patents (USSN: 10,550,570, USSN: 10,607,112, USSN: 10,004,471 USSN: 10,254,358, USSN: 10,398,399, USSN: 10,650,515, USSN: 8,774,479, USSN: 8,295,575, USSN: 8,442,285, USSN: 9,159,128, USSN: 9,177,104 B2, USSN: 9,235,887 USSN: 9,262,583, USSN: 9,483,822, USSN: 9,767,555) and 1 pending patent (CWRUP139US). His technology has been licensed (USSN: 8,442,285; USSN: 8,442,285) to Elucid Bioimaging. He is also involved in a NIH U24 grant with PathCore Inc, and 3 different R01 grants with Inspirata Inc.

Data sharing

The radiomic features generated during the current study with analysis code are available in https://github.com/lynli/RadClip.

Acknowledgements

Research reported in this publication was supported by the National Cancer Institute under award numbers 1U24CA199374-01, R01CA202752-01A1, R01CA208236-01A1, R01CA216579-01A1, R01CA220581-01A11U01CA239055-01, 1U01CA248226-01, 1U54CA254566-01; National Heart, Lung and Blood Institute 1R01HL15127701A1, National Institute for Biomedical Imaging and Bioengineering 1R43EB028736-01; National Center for Research Resources under award number 1 C06 RR12463-01; VA Merit Review Award IBX004121A from the United States Department of Veterans Affairs Biomedical Laboratory Research and Development Servicethe Office of the Assistant Secretary of Defense for Health Affairs, through the Breast Cancer Research Program (W81XWH-19-1-0668), the Prostate Cancer Research Program (W81XWH-15-1-0558, W81XWH-20-1-0851) the Lung Cancer Research Program (W81XWH-18-1-0440, W81XWH-20-1-0595), the Peer Reviewed Cancer Research Program (W81XWH-18-1-0404), the Kidney Precision Medicine Project (KPMP) Glue Grantthe Ohio Third Frontier Technology Validation Fundthe Clinical and Translational Science Collaborative of Cleveland (UL1TR0002548) from the National Center for Advancing Translational Sciences (NCATS) component of the National Institutes of Health and NIH roadmap for Medical Research. The Wallace H. Coulter Foundation Program in the Department of Biomedical Engineering at Case Western Reserve University. The DOD Prostate Cancer Idea Development Award: W81XWH-18-1-0524. Verena C Obmann received funding from the Swiss National Science Foundation, Early Postdoc Mobility fellowship grant, P2SKP3_178132.

The content is solely the responsibility of the authors and does not necessarily represent the official views of the National Institutes of Health, the U.S. Department of Veterans Affairs, the Department of Defense, or the United States Government.

References

[1] Tourinho-Barbosa R, Srougi V, Nunes-Silva I, Baghdadi M, Rembeyo G, Eiffel SS, et al. Biochemical recurrence after radical prostatectomy: what does it mean? Int Braz J Urol Off J Braz Soc Urol 2018;44(1):14–21.
[2] Freedland SJ, Humphreys EB, Mangold LA, Eisenberger M, Dorey FJ, Walsh PC, et al. Risk of prostate cancer–specific mortality following biochemical recurrence after radical prostatectomy. JAMA 2005 Jul 27;294(4):433–9.
[3] Williams S. Surrogate endpoints in early prostate cancer research. Transl Androl Urol 2018 Jun;7(3):472–82.
[4] Van den Broeck T, van den Bergh RCN, Arfi N, Gross T, Moris L, Briers E, et al. Prognostic value of biochemical recurrence following treatment with curative intent for prostate cancer: a systematic review. Eur Urol 2019 Jun 1;75(6):967–87.
[5] Patel HD, Tosoian JJ, Carter HB, Epstein JI. Adverse pathologic findings for men electing immediate radical prostatectomy: defining a favorable intermediate-risk group. JAMA Oncol 2018 Jan 1;4(1):89–92.
[6] Bloom KD, Richie JP, Schultz D, Renshaw A, Saegaert T, D'amico AV. Invasion of seminal vesicles by adenocarcinoma of the prostate: PSA outcome determined by preoperative and postoperative factors. Urology 2004 Feb 1;63(2):333–6.
[7] Mikel Hubanks J, Boorjian SA, Frank I, Gettman MT, Houston Thompson R, Rangel LJ, et al. The presence of extracapsular extension is associated with an increased risk of death from prostate cancer after radical prostatectomy for patients with seminal vesicle invasion and negative lymph nodes. Urol Oncol Semin Orig Investig 2014 Jan 1;32(1):26.e1–7.
[8] Kim HL, Li P, Huang H-C, Deheshi S, Marti T, Knudsen B, et al. Validation of the Decipher Test for predicting adverse pathology in candidates for prostate cancer active surveillance. Prostate Cancer Prostatic Dis 2019 Sep;22(3):399–405.
[9] Cooperberg MR, Hilton JF, Carroll PR. The CAPRA-S score. Cancer. 117 (22):5039–46.
[10] Brajtbord JS, Leapman MS, Cooperberg MR. The CAPRA Score at 10 years: contemporary perspectives and analysis of supporting studies. Eur Urol 2017 May 1;71 (5):705–9.
[11] Erho N, Crisan A, Vergara IA, Mitra AP, Ghadessi M, Buerki C, et al. Discovery and validation of a prostate cancer genomic classifier that predicts early metastasis following radical prostatectomy. PLOS ONE 2013 Jun 24;8(6):e66855.
[12] Ross AE, Johnson MH, Yousefi K, Davicioni E, Netto GJ, Marchionni L, et al. Tissue-based genomics augments post-prostatectomy risk stratification in a natural history cohort of intermediate- and high-risk men. Eur Urol 2016 Jan 1;69(1):157–65.
[13] Ahmed HU, El-Shater Bosaily A, Brown LC, Gabe R, Kaplan R, Parmar MK, et al. Diagnostic accuracy of multi-parametric MRI and TRUS biopsy in prostate cancer (PROMIS): a paired validating confirmatory study. The Lancet 2017 Feb 25;389 (10071):815–22.
[14] Marenco J, Orczyk C, Collins T, Moore C, Emberton M. Role of MRI in planning radical prostatectomy: what is the added value? World J Urol 2019 Jul 1;37(7):1289–92.
[15] Hegde JV, Demanes DJ, Veruttipong D, Raince J, Park S-J, Raman SS, et al. Pretreatment 3T multiparametric MRI staging predicts for biochemical failure in high-risk prostate cancer treated with combination high-dose-rate brachytherapy and external beam radiotherapy. Brachytherapy 2017 Nov 1;16(6):1106–12.
[16] Wibmer A, Vargas HA, Donahue TF, Zheng J, Moskowitz C, Eastham J, et al. Diagnosis of extracapsular extension of prostate cancer on prostate mri: impact of second-opinion readings by subspecialized genitourinary oncologic radiologists. Am J Roentgenol 2015 Jun 23;205(1):W73–8.

[17] Shiradkar R, Ghose S, Jambor I, Taimen P, Ettala O, Purysko AS, et al. Radiomic features from pretreatment biparametric MRI predict prostate cancer biochemical recurrence: Preliminary findings. J Magn Reson Imaging 2018;48(6):1626–36.
[18] Hectors SJ, Cherny M, Yadav KK, Beksaç AT, Thulasidass H, Lewis S, Davicioni E, Wang P, Tewari AK, Taouli B. Radiomics features measured with multiparametric magnetic resonance imaging predict prostate cancer aggressiveness. The Journal of urology 2019 Sep;202(3):498–505.
[19] Bourbonne V, Vallières M, Lucia F, Doucet L, Visvikis D, Tissot V, Pradier O, Hatt M, Schick U. MRI-derived radiomics to guide post-operative management for high-risk prostate cancer. Frontiers in Oncology 2019;9:807.
[20] Abdollahi H, Mofid B, Shiri I, Razzaghdoust A, Saadipoor A, Mahdavi A, et al. Machine learning-based radiomic models to predict intensity-modulated radiation therapy response, Gleason score and stage in prostate cancer. Radiol Med (Torino) 2019 Jun;124(6):555–67.
[21] Pound CR, Partin AW, Eisenberger MA, Chan DW, Pearson JD, Walsh PC. natural history of progression after PSA elevation following radical prostatectomy. JAMA 1999 May 5;281(17):1591–7.
[22] Pieper S, Halle M, Kikinis R. 3D Slicer. In: Proceedings of the 2nd IEEE international symposium on biomedical imaging: nano to macro (IEEE Cat No 04EX821), 1; 2004. p. 632–5.
[23] Sled JG, Zijdenbos AP, Evans AC. A nonparametric method for automatic correction of intensity nonuniformity in MRI data. IEEE Trans Med Imaging 1998 Feb;17(1):87–97.
[24] Juntu J, Sijbers J, Van Dyck D, Gielen J. Bias Field Correction for MRI Images. In: Kurzyński M, Puchała E, Woźniak M, żołnierek A, editors. Computer recognition systems. Berlin Heidelberg: Springer; 2005. p. 543–51.
[25] Fogel I, Sagi D. Gabor filters as texture discriminator. Biol Cybern 1989 Jun 1;61(2):103–13.
[26] Laws KI. Textured image segmentation. University of Southern California Los Angeles Image Processing INST; 1980 Jan.
[27] Haralick RM, Shanmugam K, Dinstein I. Textural features for image classification. IEEE Trans Syst Man Cybern 1973 Nov;SMC-3(6):610–21.
[28] Prasanna P, Tiwari P, Madabhushi A. Co-occurrence of local anisotropic gradient orientations (CoLlAGe): a new radiomics descriptor. Sci Rep 2016 Nov 22;6:37241.
[29] Gnep K, Fargeas A, Gutiérrez-Carvajal RE, Commandeur F, Mathieu R, Ospina JD, et al. Haralick textural features on T2 -weighted MRI are associated with biochemical recurrence following radiotherapy for peripheral zone prostate cancer. J Magn Reson Imaging JMRI 2017;45(1):103–17.
[30] Penzias G, Singanamalli A, Elliott R, Gollamudi J, Shih N, Feldman M, et al. Identifying the morphologic basis for radiomic features in distinguishing different Gleason grades of prostate cancer on MRI: Preliminary findings. PloS One 2018;13(8):e0200730.
[31] Fedorov A, Schwier M, Clunie D, Herz C, Pieper S, Kikinis R, et al. An annotated test-retest collection of prostate multiparametric MRI. Sci Data 2018 Dec 4;5:180281.
[32] Peng Hanchuan, Long Fuhui, Ding C. Feature selection based on mutual information criteria of max-dependency, max-relevance, and min-redundancy. IEEE Trans Pattern Anal Mach Intell 2005 Aug;27(8):1226–38.
[33] Weinreb JC, Barentsz JO, Choyke PL, Cornud F, Haider MA, Macura KJ, et al. PI-rads prostate imaging – reporting and data system: 2015, version 2. Eur Urol 2016 Jan 1;69(1):16–40.
[34] Vickers AJ, van Calster B, Steyerberg EW. A simple, step-by-step guide to interpreting decision curve analysis. Diagn Progn Res 2019 Oct 4;3(1):18.
[35] Vale CL, Fisher D, Kneebone A, Parker C, Pearse M, Richaud P, Sargos P, Sydes MR, Brawley C, Brihoum M, Brown C. Adjuvant or early salvage radiotherapy for the treatment of localised and locally advanced prostate cancer: a prospectively planned systematic review and meta-analysis of aggregate data. The Lancet 2020 Sep 28.
[36] Cooperberg MR, Davicioni E, Crisan A, Jenkins RB, Ghadessi M, Karnes RJ. Combined value of validated clinical and genomic risk stratification tools for predicting prostate cancer mortality in a high-risk prostatectomy cohort. Eur Urol 2015 Feb 1;67(2):326–33.
[37] Klein EA, Haddad Z, Yousefi K, Lam LLC, Wang Q, Choeurng V, et al. Decipher genomic classifier measured on prostate biopsy predicts metastasis risk. Urology 2016 Apr 1;90:148–52.
[38] Radtke JP, Takhar M, Bonekamp D, Kesch C, Erho N, du Plessis M, et al. transcriptome wide analysis of magnetic resonance imaging-targeted biopsy and matching surgical specimens from high-risk prostate cancer patients treated with radical prostatectomy: the target must be hit. Eur Urol Focus 2018 Jul 1;4(4):540–6.
[39] Purysko AS, Magi-Galluzzi C, Mian OY, Sittenfeld S, Davicioni E, du Plessis M, Buerki C, Bullen J, Li L, Madabhushi A, Stephenson A. Correlation between MRI phenotypes and a genomic classifier of prostate cancer: preliminary findings. European radiology 2019 Sep;29(9):4861–70.
[40] Jambor I, Falagario U, Ratnani P, Perez IM, Demir K, Merisaari H, et al. Prediction of biochemical recurrence in prostate cancer patients who underwent prostatectomy using routine clinical prostate multiparametric MRI and decipher genomic score. J Magn Reson Imaging 2020;51(4):1075–85.
[41] Girometti R, Giannarini G, Greco F, Isola M, Cereser L, Como G, et al. Interreader agreement of PI-RADS v. 2 in assessing prostate cancer with multiparametric MRI: A study using whole-mount histology as the standard of reference. J Magn Reson Imaging 2019;49(2):546–55.